

## Superconducting Fluctuation Diamagnetism above $T_c$ in $\text{YBa}_2\text{Cu}_3\text{O}_7$ , $\text{La}_{1.8}\text{Sr}_{0.2}\text{CuO}_4$ , and $\text{Bi}_{2-x}\text{Pb}_x\text{Sr}_2\text{CaCu}_2\text{O}_{8+\delta}$

W. C. Lee, R. A. Klemm, and D. C. Johnston

Ames Laboratory—U.S. DOE and Department of Physics, Iowa State University, Ames, Iowa 50011

(Received 25 July 1988; revised manuscript received 11 April 1989)

Magnetic susceptibility data are presented for the title compounds. All show negative curvature below  $\sim 2T_c$ . Data for grain-aligned  $\text{YBa}_2\text{Cu}_3\text{O}_7$  are in excellent agreement with a new calculation of the superconducting fluctuation diamagnetism. We infer  $s$ -wave pairing and Ginzburg-Landau coherence lengths  $\xi_{ab}(0) = 13.6 \pm 0.8 \text{ \AA}$  and  $\xi_c(0) = 1.23 \pm 0.19 \text{ \AA}$ . Both of the order-parameter bands are found to be essential in the fit. Part of the above negative curvature is inferred to arise from the normal-state background.

PACS numbers: 74.20.De, 74.40.+k, 74.65.+n, 74.70.Vy

Low-frequency<sup>1-6</sup> and microwave<sup>7</sup> conductivity data above  $T_c \approx 92 \text{ K}$  as well as heat-capacity<sup>8</sup> data near  $T_c$  for  $\text{YBa}_2\text{Cu}_3\text{O}_7$  (Y 1:2:3) indicate that superconducting fluctuations are strong at temperatures  $T$  in the vicinity of  $T_c$  and above, and that the superconductivity is three dimensional. In these measurements, a strong  $T$ -dependent background is present and must be subtracted, subject to strong assumptions about the background, in order to extract the fluctuation contributions, leading to ambiguities in the derived microscopic parameters. On the other hand, these fluctuations are also observable as a diamagnetic contribution to the magnetic susceptibility  $\chi(T)$  above  $T_c$ ,<sup>9,10</sup> which is otherwise nearly independent of  $T$ .<sup>9,10</sup> Herein, we report  $\chi(T)$  data for a batch of Y 1:2:3 which we believe closely approximate the intrinsic  $\chi(T)$ . The data increase monotonically with  $T$  up to at least 400 K, and exhibit negative curvature below  $\sim 200 \text{ K}$ . We present the results of a new calculation of the angular dependence of the superconducting fluctuation diamagnetism (SFD) and compare the predictions with our  $\chi(T)$  data for a highly oriented powder with  $\mathbf{H} \parallel \mathbf{c}$  and  $\mathbf{H} \perp \mathbf{c}$ . This comparison shows that the data are consistent with  $s$ -wave pairing and strong SFD up to at least 126 K, and provides quantitative estimates of the  $T=0$  coherence lengths and the effective mass anisotropy. We infer that the background  $\chi(T)$  exhibits negative curvature above  $T_c$ . Powder  $\chi(T)$  data are also reported for  $\text{La}_{1.8}\text{Sr}_{0.2}\text{CuO}_{3.96}$  (LaSr 2:1:4) and  $\text{Bi}_{2-x}\text{Pb}_x\text{Sr}_2\text{CaCu}_2\text{O}_{8+\delta}$  (2:2:1:2) for  $x=0$  and  $x=0.2$  which show that the strong SFD is a universal property of the copper-oxide-based materials.

Polycrystalline  $\text{YBa}_2\text{Cu}_3\text{O}_{7-y}$  was prepared from predried Ames Laboratory  $\text{Y}_2\text{O}_3$ , 99.999% CuO and 99.9%  $\text{BaCO}_3$  at  $940^\circ\text{C}$  for 90 d in air with ten intermediate grindings, followed by heating in  $\text{O}_2$  at  $640^\circ\text{C}$  for 1 d and oven cooling. From x-ray diffraction analysis, the batch was single phase with  $y \approx 0$ . Magnetization  $M$  data were obtained in a magnetic field  $H$  using a quantum design SQUID magnetometer. The small (corresponding to  $\approx 3 \text{ ppm Fe/Cu}$ ) ferromagnetic im-

purity contribution to  $M$  was determined from  $M(H)$  isotherms and is corrected below. Meissner effect  $M/H$  measurements in  $H=50 \text{ G}$  gave 48% of  $-1/4\pi$  at 10 K with a zero-field-cooled value in the same  $H$  of 127%, both uncorrected for demagnetization factors. The Meissner effect attained 10% and 50% of its maximum value at 91.4 and 88.1 K, respectively. Zero resistance was observed at 91.5 K.  $M(T)$  data for  $\mathbf{H} \parallel \mathbf{c}$  and  $\mathbf{H} \perp \mathbf{c}$  were obtained on grain-aligned free-flowing powder. Grain alignment was achieved *in situ* in the magnetometer as described elsewhere,<sup>11</sup> essentially complete alignment was achieved.<sup>11</sup>

$\chi(T)$  data in  $H=3 \text{ kG}$  are shown in Fig. 1 for Y 1:2:3. This sample shows no clear indication of the anomalies at 220–240 and/or 310 K we see in other samples from the same batch<sup>11</sup> and is seen in several other  $\chi(T)$  studies<sup>9,12</sup> of Y 1:2:3. The region of negative curvature below  $\approx 200 \text{ K}$  in Fig. 1 suggests the onset of either filamentary superconductivity or SFD in the sample.

In order to compare our results with theory, the Lawrence-Doniach<sup>13</sup> (LD) model was generalized to a magnetic field  $\mathbf{B}$  at an arbitrary angle  $\theta$  with respect to the  $c$  axis, where the influence of local clean limit dy-

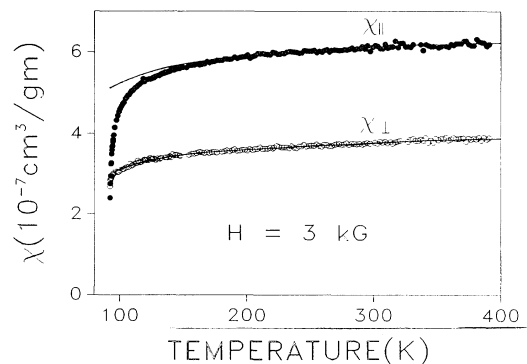


FIG. 1. Magnetic susceptibility  $\chi$  vs temperature for  $\text{YBa}_2\text{Cu}_3\text{O}_7$ . The solid curves are normal-state backgrounds (see text).

namics has also been accounted for.<sup>14</sup> In this model, there are  $N$  conducting layers per unit cell, with  $N=1$  equal interlayer spacings  $d$  and one different spacing  $d'$  ( $N=2$  for Y 1:2:3), and one complex  $s$ -wave order parameter per layer; the  $c$ -axis unit-cell edge  $s=d'+(N-1)d$ . The layers are coupled by Josephson-type tunneling, with parameters  $\zeta_1$  and  $\zeta_2$ , respectively. The Gaussian fluctuation free energy is diagonalized, yielding  $N$ -order parameter bands (in terms of their  $c$ -axis dispersions), with  $N$  distinct  $T_c$  values. Just above the highest  $T_c$ , the fluctuations are dominated by the three-dimensional (3D) regime of a single cellular order pa-

rameter. In the 2D regime further above  $T_c$ , more of the order parameters contribute to the fluctuations, with their relative contributions depending upon the  $\zeta_1$  and  $\zeta_2$  values. The weak-field regime is defined by  $\omega_c \tau_\phi \ll 1$  and  $B < B_0 \equiv \phi_0 / s v_F \tau_\phi$ , where  $\omega_c$ ,  $\tau_\phi$ , and  $v_F$  are, respectively, the pair cyclotron resonance frequency, phase coherence lifetime, and intralayer Fermi velocity. In twinned Y 1:2:3, the intertwin distance is usually  $\lesssim 1500$  Å. We therefore take  $v_F \tau_\phi$  to be  $\lesssim 1$  μm, which implies  $B_0 \gtrsim 17$  kG, so our measurements are in the weak-field regime.

In the limit  $B \rightarrow 0$ , the angular dependence of the SFD above  $T_c$  is  $\chi(\theta, T) = \chi_c(T) \cos^2 \theta + \chi_{ab}(T) \sin^2 \theta$ , where<sup>14</sup> by the standard techniques<sup>15</sup> for  $N=2$ ,

$$\chi_c(T) = \frac{-16\xi_{ab}^2(0)}{3\pi^2 s \phi_0^2} \sum_{n=0,1} k_B T_{cn} \int_0^\infty \frac{\tilde{\omega} d\tilde{\omega}}{e^{\tilde{\omega}} - 1} \int_0^\pi \frac{dq}{\tilde{\omega}^2 + [B_n(T) + C_n(T)\bar{\lambda}_n(q)]^2} \quad (1)$$

and

$$\chi_{ab}(T) = \frac{-2m\xi_{ab}^2(0)}{3M\xi_c(0)\phi_0^2\sqrt{\pi}} \sum_{n=0,1} k_B (T T_{cn})^{1/2} \int_0^\infty \frac{d\tilde{\omega} \{[\tilde{\omega}^2 + B_n^2(T)]^{1/2} - B_n(T)\}^{1/2}}{(e^{\tilde{\omega}} - 1)[\tilde{\omega}^2 + B_n^2(T)]^{1/2}}, \quad (2)$$

where

$$B_n(T) = (8T_{cn}/\pi T) \ln(T/T_{cn}), \quad (3)$$

$$C_n(T) = 16T_{cn} M \xi_c^2(0) / \pi T \hbar^2, \quad (4)$$

and

$$\bar{\lambda}_n(q) = \zeta_1 + \zeta_2 \pm [\zeta_1^2 + \zeta_2^2 + 2\zeta_1\zeta_2 \cos(q)]^{1/2} \quad (5)$$

are the order-parameter band energies in terms of  $q = k_z s$  and the Josephson coupling parameters  $\zeta_1$  and  $\zeta_2$ , where  $n=0$  (1) corresponds to  $-$  ( $+$ ) for the two order-parameter bands, and where the transition temperature  $T_{c1}$  for the upper band is given by

$$(T_{c1}/T_{c0}) \ln(T_{c0}/T_{c1}) = 4m\xi_{ab}^2(0) \hbar^{-2} \max\{\zeta_1, \zeta_2\}. \quad (6)$$

The coherence lengths  $\xi_{ab}(T) = \xi_{ab}(0) [\ln(T/T_{c0})]^{-1/2}$  and  $\xi_c = \xi_{ab} \sqrt{\epsilon}$ , where  $\epsilon = m/M$  is the ratio of pair effective masses parallel and perpendicular to the  $a$ - $b$  plane, and  $\phi_0$  is the flux quantum  $hc/2e$ .  $M$  is given by  $\hbar^2(1/\zeta_1 + 1/\zeta_2)/s^2$  in terms of microscopic tunneling parameters. We define  $\gamma \equiv \zeta_1\zeta_2/(\zeta_1 + \zeta_2)^2$ , so that  $0 \leq \gamma \leq \frac{1}{4}$ . The above system of equations is exact in the low-field regime within the framework of the time-dependent Ginzburg-Landau theory, which is accurate in the entire Gaussian fluctuation regime, neglecting scattering effects. Note that with dynamic effects included in the calculation, there is not distinct dimensional crossover between 2D and 3D  $T$  dependences, in contrast to predictions<sup>13,15</sup> when these effects are neglected. Indeed, the dynamic effects can yield a  $T$  dependence similar to that previously expected<sup>13,15</sup> for dimensional crossover even when dimensional crossover does not occur ( $\mathbf{H} \perp \mathbf{c}$ ).<sup>14</sup> We note that in our theory we have neglected any coupling of the normal-state  $\chi_{ii}(T)$  to the fluctuating superconducting order parameter.

In comparing our theory with the data in Fig. 1, it should be borne in mind that the  $\chi_{ii}(T)$  data contain

possible  $T$ -dependent contributions from normal-state background antiferromagnetic spin correlations<sup>9,16</sup> and crystallographic and/or electronic changes (see below), and from small amounts ( $\approx 0.1\%$ <sup>11</sup>) of magnetic impurity phases. Consider the anisotropy  $\Delta\chi \equiv \chi_{\parallel c} - \chi_{\perp c}$  derived from Fig. 1 and shown in Fig. 2. The first (spin-correlation) contribution should be absent in  $\Delta\chi$ , since it is essentially isotropic. From Fig. 2,  $\Delta\chi \equiv \Delta\chi_0 = 2.32 \times 10^{-7} \text{ cm}^3/\text{g}$  is constant within experimental error above 250 K, suggesting that the anisotropy of the normal-state background is independent of  $T$ . The quantity  $\delta\chi(T) \equiv \Delta\chi(T) - \Delta\chi_0$ , plotted in the inset of Fig. 2, is thus expected to contain only the SFD contribution of present interest, and we therefore fit  $\delta\chi(T)$  with the

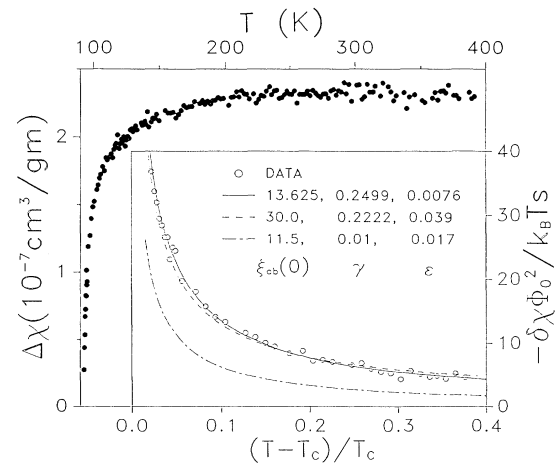


FIG. 2.  $\Delta\chi \equiv \chi_{\parallel c} - \chi_{\perp c}$  from Fig. 1 vs temperature. Inset: Plot of  $\delta\chi \equiv \Delta\chi - \Delta\chi_0$  vs  $(T - T_c)/T_c$ ; the solid curve is our optimum fit to the data and the other two curves are for nonoptimum fits.

above theory. Heat-capacity measurements on our sample<sup>11</sup> gave  $T_c = 90.8$  K, which is not an adjustable parameter in the fits below.

Theoretically predicted  $\delta\chi(T)$  curves were computed numerically for  $\gamma$  values between 0.01 and 0.2499,  $\epsilon$  values of 0.001 to 0.04, and  $\xi_{ab}(0)$  values of 10 to 30 Å. The calculations were compared with the data on a plot of  $\log_{10}[-\delta\chi/T]$  vs  $\log_{10}[\ln(T/T_c)]$  for  $T < 126$  K, and the standard deviation  $\sigma$  for each set of parameter values was computed. At fixed  $\xi_{ab}(0)$  and  $\gamma$ ,  $\epsilon$  was varied to give the minimum  $\sigma$  (Fig. 3). Fits with  $\sigma \leq 0.035$  were judged acceptable; fits with  $\sigma = 0.044$  were noticeably worse. For combinations of the three parameters yielding  $\sigma > 0.035$ , the fits showed systematic deviations from the data over appreciable ranges of  $T$  and were deemed unacceptable. The combinations of parameters which gave acceptable fits to the data in Fig. 2 are  $\xi_{ab}(0) = 13.6 \pm 0.8$  Å,  $\gamma = 0.20 \pm 0.05$ , and  $\epsilon = 0.0076 \pm 0.0015$ . For these parameter ranges, both order-parameter bands have nonzero  $T_c$  values [see Eq. (6)] and both therefore contribute to the SFD. Our optimum fit ( $\sigma = 0.027$ ) is given by the solid curve in the inset of Fig. 2. Regions of  $\xi_{ab}(0)$  values between 17 and  $\sim 25$  Å and below 12 Å are clearly unacceptable ( $\sigma > 0.07$ ). However,  $\xi_{ab}(0)$  values near 30 Å are almost acceptable ( $\sigma = 0.038$ ) if  $\gamma \approx \frac{1}{4}$ , as shown in the inset of Fig. 2. Such large values of  $\xi_{ab}(0)$  are, however, inconsistent with recent dc  $M(T)$  measurements<sup>17</sup> of  $dH_{c2}/dT$  at  $T_c$  for  $H \parallel c$ , which give  $\xi_{ab}(0) \approx 13.8$  Å. A further prediction of  $\delta\chi(T)$  for  $\xi_{ab}(0) = 11.5$  Å,  $\xi_c(0) = 1.5$  Å, and  $\gamma = 0.01$ , parameters derived<sup>18</sup> from recent fits (excluding dynamics) to paraconductivity data, is shown in the inset of Fig. 2; these parameters are obviously not consistent with our  $\delta\chi(T)$  data.<sup>18</sup>

From a log-log plot of the inset of Fig. 2, the slope of which is  $\approx -\frac{1}{2}$  for the data points near to  $T_c$  (indicative of 3D behavior), we infer that the width of the critical region is less than 1 K, consistent with previous re-

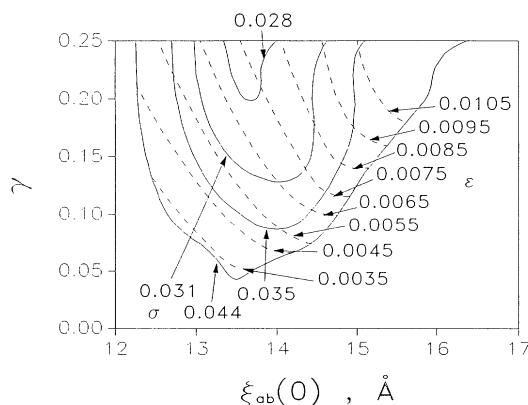


FIG. 3.  $\gamma$  vs  $\xi_{ab}(0)$ , optimized with respect to  $\epsilon$ , with contours of constant  $\epsilon = m/M$  and of constant standard deviation  $\sigma$  of the fit of theory from the data.

ports.<sup>1-5,7,8</sup> While the slope on a log-log plot in the regime  $110 < T < 126$  K is approximately  $-1$ , naively (i.e., in a static calculation) indicative of 2D behavior in that region, this interpretation is complicated by the dynamic effects present in our theory<sup>14</sup> (see above). Our ratio  $1/\epsilon = M/m \sim 100$  to 150 is consistent with some<sup>19</sup>  $H_{c2}$  anisotropy data near  $T_c$  which indicate  $M/m \sim 70$ -120. For these  $\epsilon$  values, one would expect dimensional crossover in  $\chi_c(T)$  [but not in  $\chi_{ab}(T)$ ] to occur in the  $T$  regime pictured in the inset of Fig. 2.

The background  $\chi(T)$  for  $H \parallel c$  and  $H \perp c$  was determined by subtracting the above optimal SFD contributions from the data in Fig. 1, yielding the solid curves in Fig. 1. Both backgrounds exhibit negative curvature below  $\sim 130$  K; for  $H \perp c$ , most of the observed curvature in the data arises from the  $T$ -dependent background. This observation supports numerous other studies which indicate that some sort of structural, magnetic and/or electronic modification of Y 1:2:3 occurs with decreasing  $T$  below  $\sim 130$  K.<sup>20</sup> If the negative curvature in the normal-state  $\chi_{ii}(T)$  background turns out to be anisotropic, then the parameters derived from our fits would have to be modified somewhat. Additionally, whatever sources are giving rise to the derived temperature-dependent background may also be causing the parameters of our model to be dependent on temperature.

The structures of the various Cu-O superconductors are similar in that they all contain  $\text{CuO}_2$  layers. Therefore, we expected and found the magnitudes of the SFD to be similar, as shown in Fig. 4 for LaSr 2:1:4 and 2:2:1:2; in each case the region of negative curvature (attributed in part to the SFD) begins at about  $2T_c$  as in Y 1:2:3.

In conclusion, we have presented  $\chi(T)$  data for Y 1:2:3 which show the lowest levels of paramagnetic im-

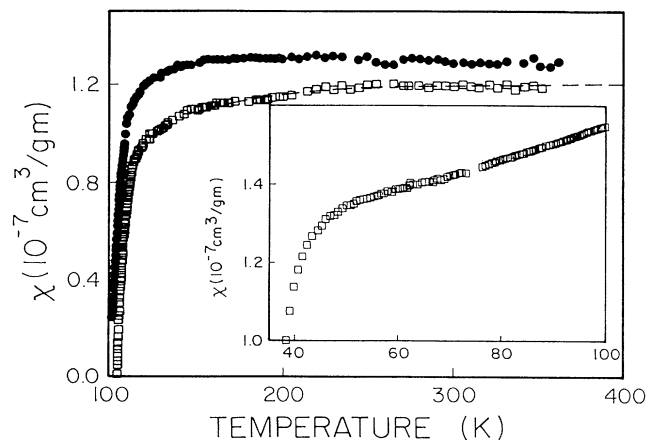


FIG. 4. Powder susceptibility  $\chi$  vs temperature for  $\text{La}_{1.8}\text{Sr}_{0.2}\text{CuO}_{3.96}$  (inset: data from Refs. 9 and 16) and  $\text{Bi}_{2-x}\text{Pb}_x\text{Sr}_2\text{CaCu}_2\text{O}_{8+\delta}$  with  $x = 0$  (circles) and 0.2 (squares).

purities or defects reported to date. The observed intrinsic  $\chi(T)$  is found to increase monotonically with  $T$ , with negative curvature below  $\sim 200$  K. This negative curvature has been directly observed without Curie-term corrections in Y 1:2:3 samples by other groups.<sup>10,21</sup> However, most published data either increase with decreasing temperature as in the early studies,<sup>22</sup> or are nearly independent of temperature above  $T_c$ ;<sup>23</sup> we infer that these behaviors are not intrinsic and are due to the presence of significant amounts of magnetic defect-impurity phases. The torque magnetometer study of single crystals by Miljak, Collin, and Hamzic<sup>12</sup> yielded  $\Delta\chi(T)$  behavior very similar to our data in Fig. 2, even though the individual  $\chi_{ii}(T)$  increased with decreasing  $T$ . We find that part but not all of the negative curvature arises from SFD. The remainder arises from a  $T$ -dependent background; this is likely reflected in the backgrounds of other properties such as the conductivity,<sup>1-6</sup> which may significantly alter the interpretation of the influence of superconducting fluctuations on these properties. Our analysis is consistent with a superconducting order parameter with  $s$ -wave symmetry on each layer, as in the LD model.<sup>13-15</sup> From fits of our new theory to the  $\chi$  data, estimates of microscopic parameters were obtained.  $\chi(T)$  data for samples of Cu-O superconductors with other structures were also presented, demonstrating that large SFD, on the order of the atomic core diamagnetism for  $T \gtrsim T_c$ , is a universal feature of this class of materials.

We are grateful to O. B. Hyun for assistance with the resistance measurements and to V. Emery, R. Fuchs, and V. Kogan for helpful discussions. Ames Laboratory is operated for the U.S. Department of Energy by Iowa State University under Contract No. W-7405-Eng-82. This work was supported by the Director for Energy Research, Office of Basic Energy Sciences.

<sup>1</sup>P. P. Freitas, C. C. Tsuei, and T. S. Plaskett, Phys. Rev. B **36**, 833 (1987).

<sup>2</sup>M. A. Dubson *et al.*, in *Novel Superconductivity*, edited by S. A. Wolfe and V. Z. Kresin (Plenum, New York, 1987), p. 981.

<sup>3</sup>N. Goldenfeld, P. D. Olmsted, T. A. Friedmann, and D. M. Ginsberg, Solid State Commun. **65**, 465 (1988); T. A. Friedmann, J. P. Rice, and D. M. Ginsberg (unpublished).

<sup>4</sup>B. Oh *et al.*, Phys. Rev. B **37**, 7861 (1988).

<sup>5</sup>F. Vidal *et al.*, Solid State Commun. **66**, 421 (1988).

<sup>6</sup>N. P. Ong *et al.*, Physica (Amsterdam) **153-155C**, 1072 (1988); S. J. Hagen, Z. Z. Wang, and N. P. Ong, Phys. Rev. B **38**, 7137 (1988).

<sup>7</sup>A. Porch, J. R. Waldram, and L. Cohen, J. Phys. F **18**, 1547 (1988).

<sup>8</sup>S. E. Inderhees *et al.*, Phys. Rev. Lett. **60**, 1178 (1988); **60**, 2445(E) (1988).

<sup>9</sup>C. Johnston, S. K. Sinha, A. J. Jacobson, and J. M. Newsam, Physica (Amsterdam) **153-155C**, 572 (1988); (unpublished).

<sup>10</sup>K. Kanoda *et al.*, Physica (Amsterdam) **153-155C**, 749 (1988); J. Phys. Soc. Jpn. **57**, 1554 (1988).

<sup>11</sup>W. C. Lee *et al.* (unpublished).

<sup>12</sup>S.-W. Cheong *et al.*, Phys. Rev. B **36**, 3913 (1987); M. Miljak, G. Collin, and A. Hamzic (unpublished).

<sup>13</sup>W. E. Lawrence and S. Doniach, in *Proceedings of the Twelfth International Conference on Low Temperature Physics, Kyoto, 1970*, edited by E. Kanda (Keigaku, Tokyo, 1971), p. 361.

<sup>14</sup>R. A. Klemm (unpublished).

<sup>15</sup>R. A. Klemm, M. R. Beasley, and A. Luther, Phys. Rev. B **8**, 5072 (1973); R. A. Klemm, Ph.D. thesis, Harvard University, 1974 (unpublished); A. Schmid, Phys. Rev. **180**, 527 (1969).

<sup>16</sup>D. C. Johnston, Phys. Rev. Lett. **62**, 957 (1989).

<sup>17</sup>U. Welp *et al.*, Phys. Rev. Lett. **62**, 1908 (1989).

<sup>18</sup>A. G. Aronov, S. Hikami, and A. I. Larkin, Phys. Rev. Lett. **62**, 965 (1989). Note that all these authors assumed  $N=1$  for Y 1:2:3 (and hence  $\gamma \ll 1$ ), and took the repeat distance  $s$  to be 12 Å (close to the value 11.7 Å used in our fits). While one could modify their theory to include both layers equally by letting  $s \rightarrow s/2$ , or roughly by letting  $\gamma \rightarrow \frac{1}{2}$ , Fig. 3 shows that those modified parameter values would still be inconsistent with our data.

<sup>19</sup>Y. Enomoto, M. Suzuki, M. Oda, and T. Murakami, Physica (Amsterdam) **148B**, 408 (1987); L. Forro, J. Y. Henry, C. Ayache, and P. Stamp, Phys. Lett. A **128**, 283 (1988); M. J. Naughton *et al.*, Phys. Rev. B **38**, 9280 (1988).

<sup>20</sup>See, e.g., W. W. Warren, Jr., *et al.*, Phys. Rev. Lett. **62**, 1193 (1989); R. P. Sharma *et al.*, *ibid.* **62**, 2869 (1989); S. Bhattacharya *et al.*, Phys. Rev. B **37**, 5901 (1988); T. Yuen *et al.*, *ibid.* **37**, 3770 (1988); P. Boolchand *et al.*, *ibid.* **37**, 3766 (1988); L. Sun *et al.*, *ibid.* **38**, 5114 (1988).

<sup>21</sup>T. R. McGuire *et al.*, Phys. Rev. B **36**, 4032 (1987).

<sup>22</sup>See, e.g., R. J. Cava *et al.*, Phys. Rev. Lett. **58**, 1676 (1987); S. Uchida, Physica (Amsterdam) **148B**, 185 (1987); D. C. Johnston *et al.*, ACS Symp. Ser. **351**, 136 (1987); S. S. P. Parkin *et al.*, Phys. Rev. B **37**, 131 (1988).

<sup>23</sup>See, e.g., R. J. Cava *et al.*, Nature (London) **329**, 423 (1987).